Enhanced solar-blind ultraviolet single-photon detection with a Geiger-mode silicon avalanche photodiode

Yafan Shi (师亚帆)[1], **Zhaohui Li** (李召辉)[1], **Baicheng Feng** (冯百成)[1], **Peiqin Yan** (颜佩琴)[1],
Bingcheng Du (杜秉乘)[1], **Hui Zhou** (周 慧)[2], **Haifeng Pan** (潘海峰)[1], and
Guang Wu (吴 光)[1,*]

[1]*State Key Laboratory of Precision Spectroscopy, East China Normal University, Shanghai 200062, China*
[2]*State Key Laboratory of Functional Materials for Informatics, Shanghai Institute of Microsystem and Information Technology, Chinese Academy of Sciences, Shanghai 200050, China*
Corresponding author: gwu@phy.ecnu.edu.cn
Received November 8, 2015; accepted January 8, 2016; posted online March 2, 2016

Solar-blind ultraviolet detection is of great importance in astronomy and industrial and military applications. Here, we report enhanced solar-blind ultraviolet single-photon detection by a normal silicon avalanche photodiode (Si APD) single-photon detector with a specially designed photon-collecting device. By re-focusing the reflected photon from the Si chip surface on the detection area by the aluminum-coated hemisphere, the detection efficiency of the Si APD at 280 nm can be improved to 4.62%. This system has the potential for high-efficiency photon detection in the solar-blind ultraviolet regime with low noise.

OCIS codes: 040.1345, 040.1880, 040.5160, 040.6040, 040.7190.
doi: 10.3788/COL201614.030401.

Due to the strong absorption of ozone gas in the stratosphere in the ultraviolet (UV) regime of 200–300 nm, solar radiation can hardly reach the Earth, which is in the so-called solar-blind UV regime. Since the background noise from solar radiation is low in this regime, important applications, such as UV astronomy[1], flame detection[2], engine monitoring, early missile threat warnings, UV imagers[3], and free-space communications[4,5], would employ photodetection at these wavelengths in order to avoid false detection and high-background noise from the sun. At present, the development of single-photon detectors in the solar-blind UV regime is focused on GaN/AlGaN avalanche photodiodes (APDs)[6–10]. The wide bandgap structure of GaN/AlGaN makes it the ideal material for UV detection[11–13], and solar-blind detection based on GaN/AlGaN APDs can be achieved without any bandpass filter by adjusting the doping concentration of Al to regulate the long-wave cut-off wavelength. The films of GaN/AlGaN are typically homoepitaxially grown on the sapphire substrates[14,15]. The lattice mismatch and the thermal expansion coefficient mismatch would cause a very high dislocation density in the films, and with the increase of the Al doping concentration, the mismatch between the AlGaN and the substrate increases, resulting in the high dark current and low efficiency of the APD devices. In recent years, as the homoepitaxial growth of the GaN film substrate has been developed, the dislocation density has been effectively reduced, leading to the possibility of fabricating APDs that can operate in the Geiger mode. The detection efficiency of such an APD device could reach 13%[16]. However, due to the fact that the dark counts of a GaN APD single-photon detector show a drastic increase with the detection area, the detection area is usually very small. Although the

detection area of the device was as small as 1075 μm^2 in Ref. [16], the dark counts were as high as 400×10^3 counts per second (cps). Recently, the detection efficiency of GaN APD has been increased to 24.3%, but the probability of dark counts is still high, up to 41%[17]. Another solution for solar-blind UV detection is based on a silicon carbide (SiC) APD with SiO$_2$ as the anti-reflection coating and the passivation layer. Generally, the thermally grown SiO$_2$ film is quite thin, preventing the SiC APD from achieving a high-voltage operation[18,19], and the anti-reflection effect is not obvious. In addition, the electric field is not evenly distributed spatially in SiC APD under a high reverse voltage. At present, besides the much lower dark counts compared to GaN APDs, the detection efficiency of a SiC APD single-photon detector could also reach 30%[20]. Compared to the above two kinds of solar-blind UV detection devices, Si APD single-photon detectors have the lowest dark counts owing to the superb crystalline quality of silicon and the mature manufacturing. For photons at wavelengths longer than 350 nm, the detection efficiency of Si APD is quite high. The maximum detection efficiency could be beyond 70%, with dark counts of less than 100 cps[21,22]. Combined with nonlinear frequency conversion, the Si APD could extend its applications in the detection of single photons into the near/mid infrared regime[23–27]. However, due to the low detection efficiency in the UV regime, the Si APD has aroused little research interest for the solar-blind UV detection. In fact, the spectral response of the Si APD could also cover the UV regime. However, in order to achieve high-efficiency detection in the visible regime, the anti-reflection coating on the Si APD surface is usually cut off around 400 nm, leaving a high reflection beyond 60% at solar-blind UV wavelengths[28,29]. Therefore, the
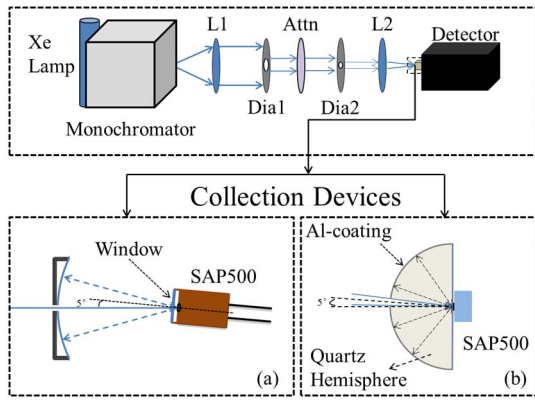
Fig. 1. Experimental setup. Xe Lamp, xenon lamp; L1, L2, UV fused silica lenses; Dia1, 2, diaphragm; Attn, attenuator. Insets: (a) Collecting device based on a concave mirror. (b) Collecting device based on a coated level hemisphere.

low detection efficiency of the Si APD in the solar-blind UV regime is partly because of the high reflection of the Si APD surface.

In this Letter, we propose and demonstrate enhanced single-photon detection at solar-blind violet wavelengths by a Si APD. By collecting the reflected photons and re-focusing them onto the detection area with a specially designed optical device, the detection efficiency of the Si APD increases to 4.62%, paving the path for a high-detection efficiency in the solar-blind UV regime with Si APDs.

Firstly, we tested the spectral response of the Si APD by a tunable light source, as shown in Fig. 1(a). The light source was an attenuated xenon lamp combined with a monochromator. We used the bandpass filters (bandwidth: 2 nm, transmittance: 50%, out of band extinction: 6OD) after the output of the monochromator to suppress the out-of-band light. None of the following measurements considered the insertion loss of the solar-blind bandpass filters, which would decrease the total detection efficiency by about 50% in a practical application. The spectral resolution of the monochromator was about 2 nm for the regime of 200–400 nm. The output from the monochromator was firstly collimated by a UV fused silica lens L1 and attenuated to 10×10^6 photons per second. It was focused on the detection area of the Si APD by another UV fused silica lens L2 with a focal length of 35 mm. The Si APD (SAP500, Laser Component GmbH) was operated in the Geiger mode at room temperature without any cooling. Therefore, the dark counts were 10×10^3 cps. The diameter of the detection area was about 500 μm. Since the Si APD was in a TO-8 package, the optical window had an anti-reflection coating for the visible regime. But the transmittance was about 70% for 214–400 nm, which was measured separately with our setup.

As shown in Fig. 2, the detection efficiency of the Si APD decreased rapidly when the light wavelength was shorter than 320 nm due to the fact that the reflection from the surface of the Si chip was above 60% in the solar-blind UV regime. There was a detection efficiency
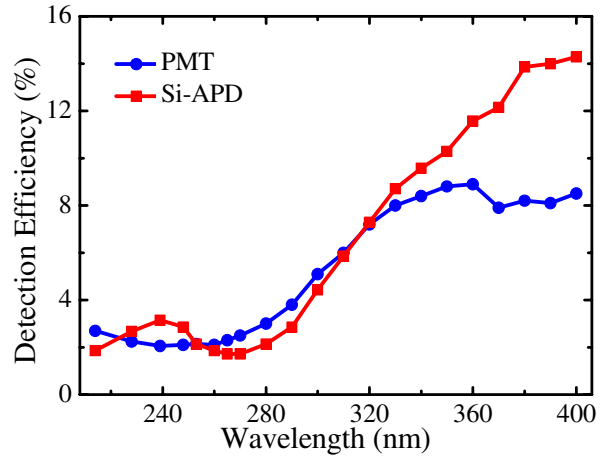

Fig. 2. Spectral response of the Si APD and the PMT.

dip at 265 nm due to the maximum reflectivity of silicon at that wavelength. Even though the detection efficiency of the Si APD was only 3.14% at 239 nm, it was better than that of the photo-multiplier tube (PMT-PM A 165-N-M, PicoQuant GmbH). Therefore, if the reflected photons from the Si chip surface could be collected and focused again on the detection area, the detection efficiency of the Si APD could be greatly increased.

To demonstrate the possibility of re-using the reflected photons, we designed a special optical structure as shown in Fig. 1(a). It was based on a concave mirror with an aluminum coating to get a high reflection of 90% in the solar-blind UV regime. A hole with diameter of 1 mm at the center of the mirror was drilled to pass the focused light onto the APD. The focal length of the concave mirror was about 9.5 mm. The Si APD was still placed at the focus of L2. It was tilted with respect to the optical axis by an angle of 5°. Then, most reflected photons would not escape through the incident hole. The optical window of the Si APD was about 1.17 mm from the surface of the Si APD chip. The concave mirror was placed about 6.5 mm from the surface of the chip so that part of the reflected photons from the surface of both the optical window and the Si APD chip could be collected and re-focused on the detection area of the Si APD. As shown in Fig. 3, an enhancement in the detection efficiency can be observed. At 350 nm, the detection efficiency increased from 10.3% to 12.3%, and at 214 nm, the detection efficiency increased from 1.86% to 1.97%. A maximum enhancement factor of 1.3 was demonstrated at 280 nm, from 2.14% to 2.79%. Considering the reflection of the optical window of about 8%, the enhancement was mainly from the re-focusing of the reflected photons from the surface of the Si APD chip by the concave mirror. With such a collection system, the detection efficiency of the Si APD in the solar-blind UV regime could be much enhanced without additional modifications to the Si APD device. Moreover, the detection efficiency in the visible regime would not be affected.

In order to further improve the collection efficiency of the reflected photons, another simple structure was designed as shown Fig. 1(b) based on a coated UV fused
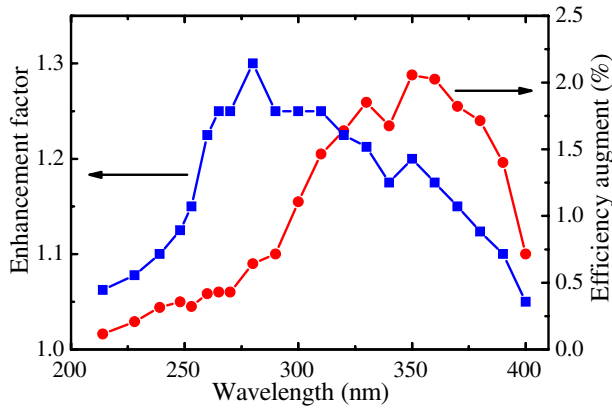
Fig. 3. Increase of the detection efficiency and the enhancement factor of the Si APD with the collecting concave mirror at different wavelengths.

silica hemisphere. The diameter of the hemisphere was about 4 mm. The surface of the hemisphere was also coated with aluminum for high reflection. A spot with a diameter of 0.5 mm at the location that was slightly off-center from the hemisphere by 5° was left uncoated for the incident photons. A Si APD (SAP-500) with a ceramic package was placed next to the plane of the hemisphere. Therefore, the detection area of the Si APD was right at the focus of the hemisphere. Theoretically, most of the reflected photons from the Si APD chip could be re-focused onto the chip according to geometrical optics, excluding the losses.

The detection efficiency of this kind of APD with a ceramic package was about 4.50% at 280 nm without the collection device. With the collection device, the detection efficiency increased to 4.62%, as shown in Fig. 4. Considering the detection efficiency without the collecting device η_0, the enhanced detection efficiency η due to i times reflection could be written as

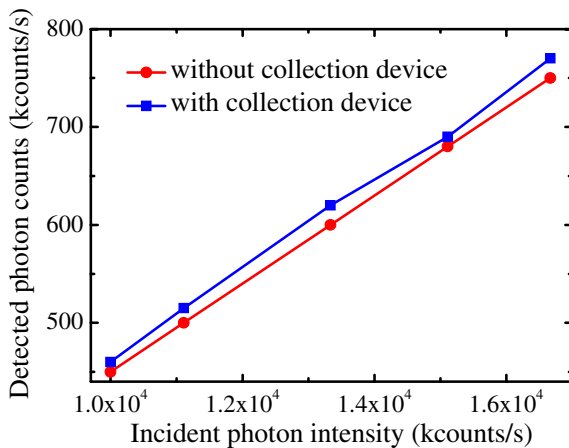$$\eta = T\eta_0 \sum_{i=0}^{i\to\infty} T^{2i} R1^i R2^i, \qquad (1)$$

Fig. 4. Si APD counting rate as a function of the incident photon intensity at 280 nm.

Table 1. Parameters of the Collecting Device and the Detection Efficiency

	T (%)	$R1$ (%)	$R2$ (%)	η_0 (%)	η (%)
Experimental	85	73	35	4.50	4.67
Optimal	100	73	90	4.50	13.11

where the transmittance of the hemisphere is T, the reflection of Si chip surface is $R1$, and the reflection of the aluminum film is $R2$. In the experiment, according to our measurements, the transmittance of the hemisphere T was about 85% at 280 nm. Since the aluminum film was not anti-oxide processed, the reflection was only about 35%. The normal incidence reflectivity of the Si was about 73%[28,29]. The enhanced detection efficiency was calculated to be 4.67% according to Eq. (1), which matches well with the experimental result of 4.62%. Therefore, further enhancement of the detection efficiency is possible by optimizing the parameter of the collecting device, as shown in Table 1. For example, the transmittance T could reach 100% by replacing the solid hemisphere with a hemisphere concave mirror. A high-reflection dielectric coating in the solar-blind UV regime could be obtained to be about 90%. Therefore, with the same Si APD, the optimized detection efficiency could be increased to 13.11%. Moreover, if the Si APD could be cooled down to −20°C, the dark noise could be reduced to below 1×10^3 cps. We did not cool the APD of the ceramic package in the experiment to avoid adding any loss for solar-blind detection. We made a cooling package detector with the same type of APD to show the performance at a low temperature. The detection efficiency was about 20% at room temperature, and increased to 50% at −20°C at 532 nm with dark counts of less than 1×10^3 cps.

In conclusion, we demonstrate that with a specially designed photon-collecting device, enhanced single-photon detection at solar-blind violet wavelengths can be realized with a normal Si APD single-photon detector. By re-focusing the reflected photon on the detection area by an aluminum-coated hemisphere, the detection efficiency of the Si APD at 280 nm increases to 4.62%. With the optimization of the collecting device, the detection efficiency will be further improved to be above 10%. This technique may provide a solution to low-noise and high-efficiency solar-blind UV detection with Si APDs.

References
1. E. Munoz, E. Monroy, F. Calle, F. Omnes, and P. Gibart, J. Geophys. Res. **105**, 4865 (2000).
2. P. Cheong, K. Chang, Y. Lai, K. Ho, I. Sou, and K. Tam, IEEE Trans. Ind. Electron. **58**, 5271 (2011).

3. J. Long, S. Varadaraajan, J. Matthews, and J. Schetzina, Opto-Electron. Rev. **10**, 251 (2002).

4. Q. He, Z. Xu, and B. Sadler, Opt. Express **18**, 12226 (2010).

5. M. Zhang, P. Luo, X. Guo, X. Zhang, D. Han, and Q. Li, Chin. Opt. Lett. **12**, 100602 (2014).

6. H. Huang, D. Yan, G. Wang, F. Xie, G. Yang, S. Xiao, and X. Gu, Chin. Opt. Lett. **12**, 092301 (2014).

7. Z. Shao, D. Chen, H. Lu, R. Zhang, D. Cao, W. Luo, Y. Zheng, L. Li, and Z. Li, IEEE Electron. Device Lett. **35**, 372 (2014).

8. L. Sun, J. Chen, J. Li, and H. Jiang, Appl. Phys. Lett. **97**, 191103 (2010).

9. Z. Vashaei, E. Cicek, C. Bayram, R. McClintock, and M. Razeghi, Appl. Phys. Lett. **96**, 201908 (2010).

10. X. Wang, W. Hu, M. Pan, L. Hou, W. Xie, J. Xu, X. Li, X. Chen, and W. Lu, J. Appl. Phys. **115**, 013103 (2014).

11. X. Feng, L. Hai, X. Xiu, D. Chen, H. Ping, Z. Rong, and Y. Zheng, Solid-State Electron. **57**, 39 (2011).

12. D. Walker, V. Kumar, K. Mi, P. Sandvik, P. Kung, X. Zhang, and M. Razeghi, Appl. Phys. Lett. **76**, 403 (2000).

13. W. Weng, T. Hsueh, S. Chang, S. Wang, H. Hsueh, and G. Huang, IEEE J. Quantum Electron. **17**, 996 (2011).

14. P. Suvarna, M. Tungare, J. Leathersich, P. Agnihotri, F. Shahedipour-Sandvik, L. Bell, and S. Nikzad, J. Electron. Mater. **42**, 854 (2013).

15. E. Tarsa, P. Kozodoy, J. Ibbetson, B. Keller, G. Parish, and U. Mishra, Appl. Phys. Lett. **77**, 316 (2000).

16. K. Mcintosh, R. Molnar, L. Mahoney, K. Molvar, N. Efremow, and S. Verghese, Appl. Phys. Lett. **76**, 3938 (2000).

17. E. Cicek, Z. Vashaei, R. McClintock, C. Bayram, and M. Razeghi, Appl. Phys. Lett. **96**, 261107 (2010).

18. Q. Zhou, D. Mcintosh, Y. Chen, Z. Li, and J. Campbell, Opt. Express **19**, 23664 (2011).

19. Q. Zhou, D. Mcintosh, Z. Lu, and J. Campbell, Appl. Phys. Lett. **99**, 131110 (2011).

20. X. Bai, H. Liu, D. Mcintosh, and J. Campbell, IEEE J. Quantum Electron. **45**, 300 (2009).

21. O. Thomas, Z. Yuan, J. Dynes, and A. Sharpe, Appl. Phys. Lett. **97**, 031102 (2010).

22. J. Youn, M. Lee, K. Park, and W. Choi, IEEE J. Quantum Electron. **48**, 229 (2012).

23. X. Gu, K. Huang, Y. Li, H. Pan, E. Wu, and H. Zeng, Appl. Phys. Lett. **96**, 131111 (2010).

24. X. Gu, K. Huang, H. Pan, E. Wu, and H. Zeng, Laser Phys. Lett. **10**, 527 (2013).

25. P. Kuo, J. Pelc, O. Slattery, Y. Kim, M. Fejer, and X. Tang, Opt. Lett. **38**, 1310 (2013).

26. D. Li, Y. Jiang, Y. Ding, I. Zotova, and N. Prasad, Appl. Phys. Lett. **101**, 141126 (2012).

27. G. Shentu, X. Xia, Q. Sun, J. Pelc, M. Fejer, Q. Zhang, and J. Pan, Opt. Lett. **38**, 4985 (2013).

28. M. A. Green, Sol. Energy Mater. Sol. Cells. **92**, 1305 (2008).

29. M. A. Green and M. J. Keevers, Prog. Photovoltaics: Res. Appl. **3**, 189 (1995).